RKKY interaction induced by two-dimensional hole gases

T. Kernreiter
School of Chemical and Physical Sciences and MacDiarmid Institute for Advanced Materials and Nanotechnology, Victoria University of Wellington, PO Box 600, Wellington 6140, New Zealand
(Received 23 May 2013; published 14 August 2013)

We analytically compute the RKKY range function as induced by two-dimensional (2D) hole gases. The bulk valence-band includes heavy-hole (HH) and light-hole (LH) states and their dynamics is described by the Luttinger Hamiltonian which we adopt as our framework. We show that even for situations where only the lowest HH-like subband is occupied the resulting form of the RKKY function can be very different as compared to the one of a 2D electron gas. The associated spin susceptibility tensor has entries along the quantum-well directions and perpendicular to it. Our formulas for the spin susceptibility tensor reveal the crucial influence of HH-LH mixing which gives rise to large anisotropies both among the in-plane components as well as among the in-plane components and the component perpendicular to the quantum well.

DOI: 10.1103/PhysRevB.88.085417 PACS number(s): 75.70.Tj, 75.75.−c, 71.10.Ca

I. INTRODUCTION

The mechanism of indirect spin interaction of nuclei[1] or magnetic impurities[2,3] mediated by conduction electrons has already been found in the 1950s and has been dubbed the Rudermann-Kittel-Kasuya-Yosida (RKKY) mechanism. The corresponding effective Hamiltonian that describes the induced spin interaction of two magnetic impurities is given by

$$\mathscr{H}^{\mathrm{RKKY}}_{\alpha\beta} = -G^2 \sum_{i,j} S_i^{(\alpha)} S_j^{(\beta)} \chi_{ij}(\mathbf{R}_\alpha, \mathbf{R}_\beta), \tag{1}$$

where $S_i^{(\alpha)}$ denotes the ith Cartesian component of an impurity spin located at position $\mathbf{R}_\alpha$, and G is the exchange constant for the contact interaction between the spin density of delocalized charge carriers with the impurity spins. In Eq. (1), $\chi_{ij}(\mathbf{R}_\alpha, \mathbf{R}_\beta)$ is the spin susceptibility which governs the form and range of the RKKY interaction and is determined by quantities of the carrier system. In the cases of an electron gas in three and two dimensions[4,5] the spin susceptibilities have a rather simple functional form with respect to the distance R between two impurities, given as

$$\chi(R) \sim \begin{cases} \frac{1}{R^3}\left[\frac{\sin(2k_F R)}{2k_F R} - \cos(2k_F R)\right] & \text{(3D)} \\ J_0(k_F R)Y_0(k_F R) + J_1(k_F R)Y_1(k_F R) & \text{(2D).} \end{cases} \tag{2}$$

Here k_F is the Fermi wave vector and $J_n(\cdot)$ and $Y_n(\cdot)$ are Bessel functions of the first and second kind, respectively. It follows from (2) that the associated Friedel oscillations decay as R^{-3} and R^{-2} for a 3D and 2D electron gas (2DEG), respectively.

Ever since its discovery, the RKKY mechanism has been studied for a large variety of systems as it allows one not only to determine the spin orientation of two isolated impurities but still more importantly to obtain valuable information about the magnetic properties of a macroscopic system. For the case of a 2DEG recent calculations have considered the influence of electron-electron interaction,[6] Rashba[7–10] spin-orbit coupling with Dresselhaus[11,12] spin-orbit coupling, and a combination of electron-electron interaction and spin-orbit couplings.[13,14] For graphene it was noticed[15,16] that Friedel oscillations decay as R^{-2} for the doped case and like R^{-3} in the undoped case.

In the case of dilute magnetic semiconductors (DMS) it has been demonstrated[17] that the experimentally found ferromagnetic order and transition temperatures can be ascribed to the RKKY mechanism. In this case, however, it is not mediated by conduction electrons but by valence holes. Subsequent theoretical studies[18–22] have considered various effects that can account for the observed magnitude of magnetization (for a recent review see Ref. 23). Also for two-dimensional DMS it has been suggested[24–29] that the RKKY mechanism accounts for observed phenomena. The RKKY interaction in such two-dimensional hole systems is often modeled in the same fashion as in the case of electrons (2), assuming a one-band effective mass approximation. Such assumptions, however, neglect the nonparabolic character[30] of hole dispersion bands and is therefore not always warranted.

Also taking into account the subtle effects due to nonparapolicity by means of a numerical subband $k \cdot p$ theory[31] calculation for a hole system based on GaAs, it has been shown[32] that the spin susceptibility tensor exhibits strong anisotropy with the variation of the carrier density. In particular, it has been pointed out that easy-plane entries of the spin susceptibility tensor can dominate over the easy-axis component. This feature was attributed to the effect of heavy hole (HH) light hole (LH) mixing which increases when the density of the hole gas is increased.

In the present paper we provide further insight into the mechanism of HH-LH mixing and its influence on the RKKY range function, where we give analytical results for the spin susceptibility tensor. This is advantageous as it allows us to retain the explicit dependence on relevant band structure parameters. We base this calculation on an effective Luttinger model,[33–36] and demonstrate that the anisotropy of the spin susceptibility tensor entries is intimately connected to the HH-LH mixed character of the hole states. Such an analytic result for the spin susceptibility tensor of two-dimensional hole gases is still missing in the literature and deviates from the simple form of an equivalent electron system [Eq. (2)].

In Sec. II we give a short account of the effective Luttinger model and define the relevant band structure parameters. In Sec. III we outline the calculation of the spin susceptibility tensor. Numerical results are presented in Sec. IV. Section V contains a short summary.

II. MODEL

In order to calculate the RKKY interaction mediated by 2D holes our starting point will be the 4×4 Luttinger model[37] as it provides a useful description of the uppermost valence band of typical semiconductors in situations where its couplings to the conduction band and split-off valence band can be neglected. We adopt the Luttinger model in axial approximation, where we neglect anisotropic terms which are usually small:

$$\mathscr{H}_L = \mathscr{H}_0 + \mathscr{H}_1 + \mathscr{H}_2, \tag{3a}$$

$$\mathscr{H}_0 = -\frac{\hbar^2}{2m_0}\left[\gamma_1\left(\mathbf{k}_\parallel^2 + k_z^2\right) + \tilde{\gamma}_1\left(\mathbf{k}_\parallel^2 - 2k_z^2\right)\left(\hat{J}_z^2 - \frac{5}{4}\mathbb{1}\right)\right], \tag{3b}$$

$$\mathscr{H}_1 = \frac{\hbar^2}{m_0}\sqrt{2}\tilde{\gamma}_2(\{k_z,k_+\}\{\hat{J}_z,\hat{J}_-\} + \{k_z,k_-\}\{\hat{J}_z,\hat{J}_+\}), \tag{3c}$$

$$\mathscr{H}_2 = \frac{\hbar^2}{2m_0}\tilde{\gamma}_3(k_+^2\hat{J}_-^2 + k_-^2\hat{J}_+^2). \tag{3d}$$

Cartesian components of the spin-3/2 matrix vector are denoted by $\hat{J}_{x,y,z}$, and we use the abbreviations $k_\pm = k_x \pm ik_y$, $\hat{J}_\pm = (\hat{J}_x \pm i\hat{J}_y)/\sqrt{2}$, and $\{A,B\} = (AB + BA)/2$. The constants γ_1 and $\tilde{\gamma}_j$ are materials-dependent band structure parameters,[38] where $\tilde{\gamma}_j$ depend also on the quantum-well growth direction and their explicit expressions in terms of the standard Luttinger parameters[37,38] γ_2 and γ_3 can be found, e.g., in Table C.10 of Ref. 39.

A potential $V(z)$ along the z direction models the confinement of holes to a 2D quantum well. In the following we assume the potential $V(z)$ to be a hard-wall confinement with width d. An effective Hamiltonian that describes the lowest size-quantized orbital bound state approximately is then obtained from (3a) by replacing $k_z \to \langle k_z\rangle = 0$ and $k_z^2 \to \langle k_z^2\rangle = (\pi/d)^2$.[33–36] In such a way we neglect HH-LH mixing among different orbital subbands. In order to absorb the width dependence of our results into prefactors, we introduce the energy scale $E_0 = -\pi^2\hbar^2\gamma_1/(2m_0d^2)$ and define wave vector components in units of π/d. Throughout this paper we will work with dimensionless wave vectors and dimensionless energies and include factors of π/d and E_0 in the calculation where it is appropriate. The (dimensionless) effective Hamiltonian is then given by

$$\mathscr{H}_L^{2D}(\mathbf{k}_\parallel) = E_0\big\{\mathbb{1} - 2\bar{\gamma}\big(\hat{J}_z^2 - \tfrac{5}{4}\mathbb{1}\big) + \big[\mathbb{1} + \bar{\gamma}\big(\hat{J}_z^2 - \tfrac{5}{4}\mathbb{1}\big)\big]\mathbf{k}_\parallel^2 - \alpha\bar{\gamma}(k_+^2\hat{J}_-^2 + k_-^2\hat{J}_+^2)\big\}, \tag{4}$$

where we define the parameters $\bar{\gamma} \equiv \tilde{\gamma}_1/\gamma_1$ and $\alpha \equiv \tilde{\gamma}_3/\tilde{\gamma}_1$ to discuss the effects of HH-LH splitting and HH-LH mixing separately. Note that for $\mathbf{k}_\parallel = 0$, the Hamiltonian (4) commutes with $\hat{J}_z$ which has eigenvalues $\pm 3/2$ (HH) and $\pm 1/2$ (LH). Their corresponding energies are split up which is described by the parameter $\bar{\gamma}$. For $\mathbf{k}_\parallel \neq 0$ (and $\alpha \neq 0$), on the other hand, the eigenstates of the Hamiltonian are not simultaneously eigenstates of $\hat{J}_z$, with α describing the effect of HH-LH mixing.

III. SPIN SUSCEPTIBILITY TENSOR

In the following we will calculate the spin susceptibility tensor for a 2D hole gas. The analytical expression for the spin susceptibility tensor in linear response theory and for finite temperature is conveniently given in terms of Matsubara Green's functions of the holes and reads[40]

$$\chi_{ij}(\mathbf{R}) = k_\mathrm{B}T\sum_n \mathrm{Tr}\big\{\hat{J}_i G_{\omega_n}(\mathbf{R})\hat{J}_j G_{\omega_n}(-\mathbf{R})\big\}, \tag{5}$$

where $\omega_n = (2n+1)\pi k_\mathrm{B}T$ are the Matsubara frequencies. In the following we will consider the case of zero temperature for which the result of the spin susceptibility tensor is straightforwardly obtained from Eq. (5) by making in the Green's functions the replacements $i\omega_n \to \omega + i\delta\,\mathrm{sgn}(\omega)$ to obtain the retarded and advanced Green's functions for zero temperature.[41] Furthermore, we have to replace the sum by an integral according to $k_\mathrm{B}T\sum_n \to \frac{1}{2\pi i}\int_{\Gamma_1} d\omega$, with the contour of the integration given by $\Gamma_1 = (-\infty - i\delta, -i\delta) \cup (i\delta, \infty + i\delta)$. The Green's function in real space is calculated by a Fourier transformation of the Green's function in momentum space, where the latter is given by

$$G_\omega(\mathbf{k}_\parallel) = \frac{1}{E_0}\big[\bar{\omega} + \varepsilon_F - \mathscr{H}_L^{2D}(\mathbf{k}_\parallel)/E_0\big]^{-1}. \tag{6}$$

Here we use the abbreviation $\bar{\omega} \equiv \omega + i\delta\,\mathrm{sgn}(\omega)$, ε_F is the Fermi energy, and again we use dimensionless quantities as $\varepsilon_F \to E_0\varepsilon_F$ and $\bar{\omega} \to E_0\bar{\omega}$.

From Eq. (6) we obtain for the Green's function in momentum space (using polar coordinates):

$$[G_\omega(\mathbf{k}_\parallel)]_{ij} = [A_-(\delta_{i1}+\delta_{i4}) + A_+(\delta_{i2}+\delta_{i3})]\delta_{ij} + B[e^{-i2\phi_k}(\hat{J}_+^2)_{ij} + e^{i2\phi_k}(\hat{J}_-^2)_{ij}], \tag{7}$$

with

$$A_\mp = \frac{1}{E_0}\frac{1 + k^2 \mp \bar{\gamma}(k^2-2) - (\bar{\omega}+\varepsilon_F)}{[\bar{\gamma}^2(1+3\alpha^2)-1]\big(k^2-k_1^2\big)\big(k^2-k_2^2\big)},$$
$$B = \frac{1}{E_0}\frac{\alpha\bar{\gamma}k^2}{[\bar{\gamma}^2(1+3\alpha^2)-1]\big(k^2-k_1^2\big)\big(k^2-k_2^2\big)}, \tag{8}$$

and δ_{ij} being the Kronecker symbol. The Green's function has poles at

$$k_{1,2} = \frac{1}{\sqrt{1-\bar{\gamma}^2(1+3\alpha^2)}}\{\bar{\omega}+\varepsilon_F - 1 - 2\bar{\gamma}^2 \mp \sqrt{(\bar{\omega}+\varepsilon_F-3)^2 + 3\alpha^2[(\bar{\omega}+\varepsilon_F-1)^2 - 4\bar{\gamma}^2]}\}^{1/2}, \tag{9}$$

which coincide with the Fermi wave vectors[35] of the two hole states for $\bar{\omega} = 0$. Thus, in order to obtain the Green's function in real space, we have to evaluate integrals of the form

$$\{\mathscr{I}, \mathscr{J}, \mathscr{K}_\pm\} = \left(\frac{\pi}{d}\right)^2\frac{1}{E_0}\int_0^{2\pi}\frac{d\phi_k}{(2\pi)^2}\int_0^\infty dk\,k \times \frac{\{1, k^2, k^2e^{\pm i2\phi_k}\}e^{ikR\cos(\phi_k-\phi_R)}}{\big(k^2-k_1^2\big)\big(k^2-k_2^2\big)}, \tag{10}$$

where we also use a dimensionless description for the distance by changing $R \to (d/\pi)R$ and with ϕ_R being the angle between the x axis and the axis given by the two impurities. We

calculate these integrals by using the Cauchy integral theorem, where we close the contour along the upper half-plane to obtain[42]

$$\begin{aligned}\mathscr{I} &= \frac{i}{4}\left(\frac{\pi}{d}\right)^2 \frac{1}{E_0}\frac{H_0^{(1)}(k_1R)-H_0^{(1)}(k_2R)}{k_1^2-k_2^2},\\ \mathscr{J} &= -\frac{i}{4}\left(\frac{\pi}{d}\right)^2 \frac{1}{E_0}\frac{k_1^2H_2^{(1)}(k_1R)-k_2^2H_2^{(1)}(k_2R)}{k_1^2-k_2^2},\\ \mathscr{K}_\pm &= -\mathscr{J}e^{\pm i2\phi_R}.\end{aligned} \tag{11}$$

Here $H_n^{(1)}(\cdot)$ denote Hankel functions of the first kind. From Eqs. (7) and (11) we find for the Green's function in real space

$$\begin{aligned}[G_\omega(\mathbf{R})]_{ij} = [\mathscr{A}_-(\delta_{i1}+\delta_{i4})+\mathscr{A}_+(\delta_{i2}+\delta_{i3})]\delta_{ij}\\ +\mathscr{B}[e^{-i2\phi_R}(\hat{J}_+^2)_{ij}+e^{i2\phi_R}(\hat{J}_-^2)_{ij}],\end{aligned} \tag{12}$$

with

$$\begin{aligned}\mathscr{A}_\mp &= \left(\frac{\pi}{d}\right)^2\frac{1}{E_0}\frac{[1\pm 2\bar{\gamma}-(\bar{\omega}+\varepsilon_F)]\mathscr{I}+(1\mp\bar{\gamma})\mathscr{J}}{\bar{\gamma}^2(1+3\alpha^2)-1},\\ \mathscr{B} &= -\left(\frac{\pi}{d}\right)^2\frac{1}{E_0}\frac{\alpha\bar{\gamma}\,\mathscr{J}}{\bar{\gamma}^2(1+3\alpha^2)-1},\end{aligned} \tag{13}$$

where we have that $G_\omega(-\mathbf{R})=G_\omega(\mathbf{R})$. Performing the trace in Eq. (5) for the various nonvanishing entries of the susceptibility tensor, yields

$$\begin{aligned}\mathrm{Tr}\{\hat{J}_xG_\omega\hat{J}_xG_\omega\} &= 3\mathscr{A}_+\mathscr{A}_-+2\mathscr{A}_+^2+9\mathscr{B}^2\\ &\quad+12\mathscr{A}_+\mathscr{B}\cos 2\phi_R, &\text{(14a)}\\ \mathrm{Tr}\{\hat{J}_yG_\omega\hat{J}_yG_\omega\} &= 3\mathscr{A}_+\mathscr{A}_-+2\mathscr{A}_+^2+9\mathscr{B}^2\\ &\quad-12\mathscr{A}_+\mathscr{B}\cos 2\phi_R, &\text{(14b)}\\ \mathrm{Tr}\{\hat{J}_xG_\omega\hat{J}_yG_\omega\} &= 12\mathscr{A}_+\mathscr{B}\sin 2\phi_R, &\text{(14c)}\\ \mathrm{Tr}\{\hat{J}_zG_\omega\hat{J}_zG_\omega\} &= \tfrac{1}{2}\left[9\mathscr{A}_-^2+\mathscr{A}_+^2-18\mathscr{B}^2\right]. &\text{(14d)}\end{aligned}$$

Due to the appearance of the last term in Eqs. (14a) and (14b) in-plane anisotropy of the RKKY interaction is introduced by HH-LH mixing ($\alpha\neq 0$) which is a distinctive feature of a 2D hole system as compared to the corresponding electron system.

To obtain the final result for the spin susceptibility tensor, we still have to integrate the terms in Eqs. (14a)–(14d) over the frequency along the contour Γ_1. For this integration, we use the method proposed in Ref. 41. Within our framework [Eq. (4)], where we assume that only the lowest HH-like subband is occupied, we can replace the integral along the contour Γ_1 by an integral along the two lines $\Gamma_2=(-i\delta,\omega_0-i\delta)\cup(\omega_0+i\delta,i\delta)$, with $\omega_0=-\varepsilon_F+1-2\bar{\gamma}$. Note that the two lines are below and above the branch cut in the complex frequency plane which corresponds to the domain (ω_0,∞), where the real part under the square root in k_2 is positive. The possibility to exchange the integration domains is a consequence of Cauchy's integral theorem which states that the integral of an analytic function over a closed curve is zero, which means in our case $\int_\cap+\int_{\Gamma_1}+\int_{\Gamma_2}=0$. The symbol $\cap$ denotes the curve in the upper half plane extended to infinity, and the corresponding integral gives zero as the Hankel functions vanish in this limit. Thus we can make the replacement $\int_{\Gamma_1}\to-\int_{\Gamma_2}$. We then evaluate all possible products of Hankel functions in Eqs. (14a)–(14d), where we find

$$\begin{aligned}&\int_{\Gamma_2}d\omega f(\omega)H_n^{(1)}(k_1R)H_m^{(1)}(k_2R)\\ &\quad= i\frac{4}{\pi}e^{-in\pi/2}\int_0^{\omega_0}d\omega f(\omega)K_n(|k_1|R)J_m(k_2R), &\text{(15a)}\\ &\int_{\Gamma_2}d\omega f(\omega)H_n^{(1)}(k_2R)H_m^{(1)}(k_2R)\\ &\quad= -2i\int_0^{\omega_0}d\omega f(\omega)[J_n(k_2R)Y_m(k_jR)+J_m(k_2R)Y_n(k_iR)], &\text{(15b)}\end{aligned}$$

for $n,m=0,2$ and $f(\omega)$ denotes an analytic function in ω. In obtaining Eq. (15b) we have used the relation $K_n(z)=\frac{i\pi}{2}e^{in\pi/2}H_n^{(1)}(ze^{i\pi/2})$ for Hankel functions that have k_1 (which is imaginary) in their argument, where $K_n(\cdot)$ are the modified Bessel functions of the second kind. In addition we have used the relation $H_n^{(1)}(ze^{i\pi})=-e^{-i\pi n}H_n^{(2)}(z)$ between Hankel functions of the first and second kind that contain k_2 and the definition of Hankel functions in terms of Bessel functions. The integrated products of Hankel functions involving only k_1 give zero. Using Eqs. (14a)–(14d) together with Eqs. (15a) and (15b) we finally obtain the (semi-)analytical result for the spin susceptibility tensor.

Considering the limit of large distances, $k_FR\gg 1$, a particular simple expression can be found for the spin susceptibility tensor, because in this case the Bessel functions can be approximated very well by

$$\begin{aligned}J_n(x) &\approx \sqrt{\frac{2}{\pi x}}\cos(x-n\pi/2-\pi/4),\\ Y_n(x) &\approx \sqrt{\frac{2}{\pi x}}\sin(x-n\pi/2-\pi/4),\end{aligned} \tag{16}$$

whereas $K_n(x)$ decays exponentially with the distance and can be approximated as $K_n(x)\approx 0$. Using these approximations and setting $\phi_R=0$, the spin susceptibility tensor elements can be given by the compact expression

$$\chi_{ii}(\mathbf{R})=\chi_0\int_0^{\omega_0}d\omega\left[\frac{a_{ii}+b_{ii}k_2^2+c_{ii}k_2^4}{\left(|k_1|^2+k_2^2\right)^2}\right]\frac{\cos(2k_2R)}{k_2R}, \tag{17}$$

with $\chi_0=2m_0\pi^2/(\hbar^2\gamma_1d^2)$ and coefficients

$$\begin{aligned}a_{xx} &= a_{yy}=Z[12\bar{\gamma}(\omega-\omega_0)-5(\omega-\omega_0)^2],\\ b_{xx,yy} &= Z\{[10+4\bar{\gamma}(1\pm 3\alpha)](\omega-\omega_0)-12\bar{\gamma}(1+\bar{\gamma})\},\\ c_{xx,yy} &= Z\{\bar{\gamma}[\bar{\gamma}-9\alpha^2\bar{\gamma}-4\mp 12\alpha(\bar{\gamma}+1)]-5\},\\ a_{zz} &= Z[36\bar{\gamma}(\omega-\omega_0)-5(\omega-\omega_0)^2-72\bar{\gamma}^2],\\ b_{zz} &= Z[2(5-4\bar{\gamma})(\omega-\omega_0)+36\bar{\gamma}(\bar{\gamma}-1)],\\ c_{zz} &= Z\{\bar{\gamma}[\bar{\gamma}(9\alpha^2-5)+8]-5\},\end{aligned} \tag{18}$$

where $Z=\frac{1}{(8\pi^2)}[(3\alpha^2+1)\bar{\gamma}^2-1]^{-2}$ and $k_{1,2}$ are given in Eq. (9) with $\bar{\omega}\to\omega$. We note that in the limit of zero HH-LH mixing, $\alpha\to 0$, we find that the elements $\chi_{xx}(\mathbf{R})=\chi_{yy}(\mathbf{R})$ decay exponentially. This can be understood from the form of the Green's function in Eq. (12) and the spin susceptibility tensor in Eqs. (14a)–(14d). As there are only HH states mediating the RKKY interaction but no mixing with LH states, only the first term in Eq. (14d) can be nonvanishing, and every

single term in the sums vanishes identically (after integration). The spin susceptibility tensor element $\chi_{zz}(\mathbf{R})$, on the other hand, is nonvanishing and coincides with the RKKY range function of a 2DEG in the limit $\alpha \to 0$.

Furthermore, we note that due to the axial symmetry of the Hamiltonian, the result for the spin susceptibility tensor for arbitrary ϕ_R is obtain by an orthogonality transformation of $\chi_{ii}(R,\phi_R = 0)$ with a rotation about the z axis with an angle ϕ_R. Of course this leaves $\chi_{zz}(\mathbf{R})$ invariant, and one simply has to transform the coefficient matrices in Eq. (17), e.g., $a_{ii} \to O \cdot \mathrm{diag}(a_{ii}) \cdot O^T$, etc.

Moreover, we find that the largest in-plane components of spin susceptibility tensor are obtained in the case where the axis connecting two localized impurities coincide with their spin-quantization axis, i.e., $|\chi_{xx}|$ is largest (smallest) for $\phi_R = 0$ ($\phi_R = \pi/2$), whereas for the magnitude of χ_{yy} the opposite relation holds.

IV. NUMERICAL RESULTS

Now we turn to a numerical analysis to study the dependence of the spin susceptibility $\chi_{ij}(\mathbf{R})$ [Eq. (5)] on the Fermi energy E_F and the band structure parameters $\bar{\gamma}$ and α. In accordance with the calculation of the spin susceptibility in the previous section, we consider only cases where only the lowest HH-like subband is occupied.

We have checked that the result based on the analytical approach given in the present paper agrees with the numerical method of calculating the spin susceptibility by means of eigenbasis functions of the Hamiltonian, i.e., by employing the Lehmann representation for the Green's functions.[35]

A. Spin susceptibility of GaAs

We start by presenting results of the RKKY range function for the case of a [001]-grown GaAs heterostructure where the corresponding band structure parameter values are $\bar{\gamma} = 0.31$ and $\alpha = 1.2$. In the following examples we vary the Fermi density $E_F = E_0 \varepsilon_F$ with the dimensionless parameters ε_F. In Fig. 1 we show $\chi_{ij}(\mathbf{R})$ (with $\phi_R = 0$) as function of $k_F R$, for the Fermi energies $\varepsilon_F = 0.9$ and $\varepsilon_F = 1.4$, respectively. In both plots, the Friedel oscillations decay as R^{-2}, which is the usual result for two-dimensional systems. By comparing Figs. 1(a) and 1(b) we see that for lower hole densities $\chi_{zz}(R)$ dominates, whereas for increased hole density $\chi_{xx}(R)$ becomes the dominant entry of the spin susceptibility tensor. In Fig. 1(b) we can also clearly see the strong influence of the HH-LH mixing parameter α which gives rise to $\chi_{xx}(R) \gg \chi_{yy}(R)$.

B. Full parameter dependence of spin susceptibility

Now we will consider scenarios where in addition to the Fermi energy the band structure parameters $\bar{\gamma}$ and α are varied. Obviously most values will not correspond to actual semiconductor materials. As we will see however, such an approach allows us to elucidate the influence of HH-LH mixing on the spin susceptibility tensor entries. Again we discuss density ranges where only the lowest HH-like subband is occupied. The next-to-lowest subband is either the lowest LH-like subband or the next-to-lowest HH-like subband. Which of the two situations is realized depends on the value of the HH-LH splitting parameter $\bar{\gamma}$, which is related to the corresponding band edge energies by $\varepsilon = 1 + 2\bar{\gamma}$ and $\varepsilon = 4(1 - 2\bar{\gamma})$, respectively. Thus we impose the following constraint on the Fermi energy: $\varepsilon_F < \min\{1 + 2\bar{\gamma}, 4(1 - 2\bar{\gamma})\}$.

To study the influence of HH-LH mixing for this general case, it is convenient to define the following HH-LH mixing angle[35]

$$\sin\theta_{\mathrm{HL}} = \frac{\sqrt{3}\alpha k_F^2}{\sqrt{3\alpha^2 k_F^4 + \left[\sqrt{3\alpha^2 k_F^4 + \left(k_F^2 - 2\right)^2} - k_F^2 + 2\right]^2}}, \tag{19}$$

which depends only on α and k_F. The Fermi wave vector k_F depends in turn on the Fermi energy ε_F and the band structure parameters $\bar{\gamma}$ and α, see Eq. (9). The modulus squared of $\sin\theta_{\mathrm{HL}}$ tells us the amount of light hole character of the lowest HH-like band and is therefore a measure for HH-LH mixing. In order to show the $\sin^2\theta_{\mathrm{HL}}$ dependence on the Fermi energy as well as on the parameters $\bar{\gamma}$ and α, we plot in Fig. 2 $\sin^2\theta_{\mathrm{HL}}$ as a function of $\bar{\gamma}$ and ε_F for $\alpha = 1.0$ (dashed lines) and $\alpha = 1.2$ (solid lines). It can be seen that $\sin^2\theta_{\mathrm{HL}}$ is monotonically increasing with ε_F, $\bar{\gamma}$, and α.

1. *Anisotropy between χ_{xx} and χ_{yy}*

Now we analyze the size of in-plane anisotropy due to HH-LH mixing, where we define the following ratio to quantify the deviation from the isotropic case:

$$r \equiv \frac{\chi_{xx}(\mathbf{R}) - \chi_{yy}(\mathbf{R})}{\chi_{xx}(\mathbf{R}) + \chi_{yy}(\mathbf{R})}. \tag{20}$$

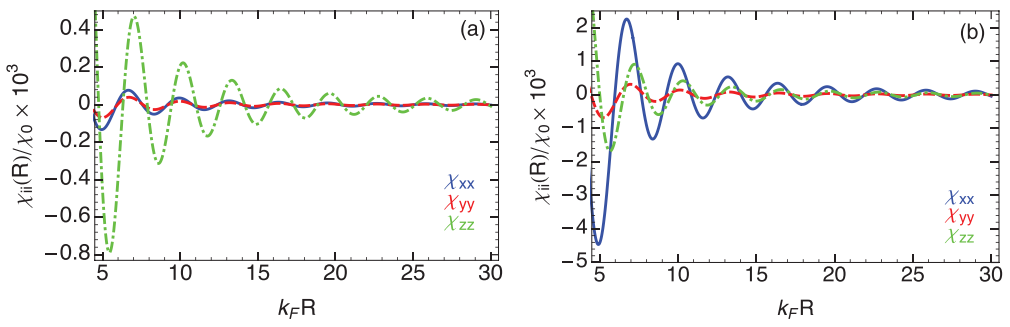

FIG. 1. (Color online) The spin susceptibility tensor entries $\chi_{ij}(\mathbf{R})$ as a function of $k_F R$ (with $\phi_R = 0$), for (a) $\varepsilon_F = 0.9$ and (b) $\varepsilon_F = 1.4$.

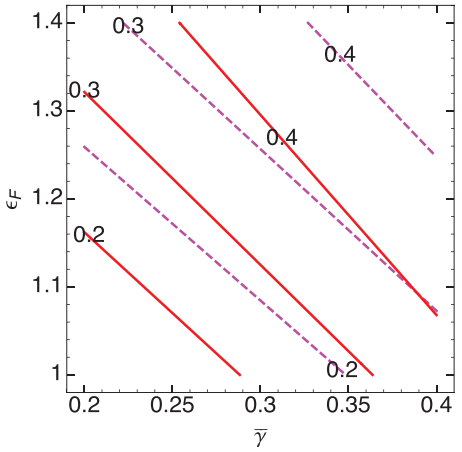

FIG. 2. (Color online) Contours of $\sin^2\theta_{\rm HL}$ [Eq. (19)] in the $\bar{\gamma}$-ε_F plane, for $\alpha = 1.0$ (dashed lines) and $\alpha = 1.2$ (solid lines).

We then randomly generate 1000 number triples of the structure parameters within their respective ranges $\bar{\gamma} \in (0.2,0.4)$ and $\alpha \in (0.9,1.4)$ and the Fermi energy in the range $\varepsilon_F \in (0.9,1.5)$. Using these number triples, we calculate r and $\sin\theta_{\rm HL}$. The result is displayed in Fig. 3, where we plot r (for $k_F R = 10$ and $\phi_R = 0$) versus $\sin^2\theta_{\rm HL}$. We find a clear correlation between the in-plane anisotropy and the HH-LH mixing angle, showing that r is a monotonically increasing function of $\sin^2\theta_{\rm HL}$. The in-plane anisotropy can go up to 90%. We note that this result is not very sensitive to the choice for $k_F R$, provided we take values in the vicinity of a maxima of the Friedel oscillations (and $k_F R \gg 1$).

2. *Anisotropy between χ_{xx} and χ_{zz}*

We have seen in Fig. 1 that the dominance between $\chi_{xx}(\mathbf{R})$ and $\chi_{zz}(\mathbf{R})$ changes with the value of the Fermi energy. This can be attributed to HH-LH mixing because by increasing the Fermi energy (density), hole states with larger wave vectors are populated which exhibit a stronger HH-LH mixing.[39] However, for Fig. 1 the band structure parameters $\bar{\gamma}$ and α were held fixed and it is not clear if other values would give rise to a different behavior. To answer this question, whether HH-LH mixing is indeed the underlying mechanism for the change from easy-axis to easy-plane dominance, we show in Fig. 4 the boundary lines of $\chi_{xx}(\mathbf{R}) = \chi_{zz}(\mathbf{R})$ in the $\bar{\gamma}$-ε_F plane for various values of α, choosing $k_F R = 10$ and $\phi_R = 0$. Below the lines we have $\chi_{zz}(\mathbf{R}) > \chi_{xx}(\mathbf{R})$ and

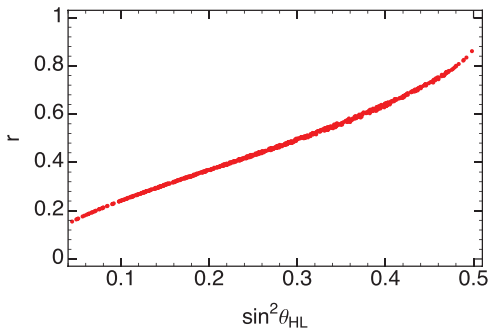

FIG. 3. (Color online) The ratio r [Eq. (20)] versus $\sin^2\theta_{\rm HL}$.

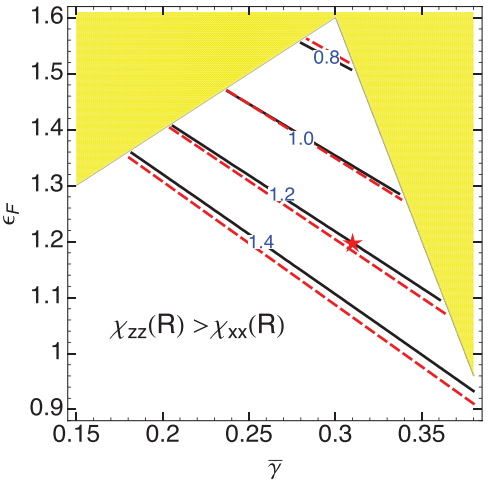

FIG. 4. (Color online) Boundaries in the $\bar{\gamma}$-ε_F plane where $\chi_{xx}(\mathbf{R}) = \chi_{zz}(\mathbf{R})$, for HH-LH mixing parameter values $\alpha = 0.8,1.0,1.2,1.4$ (black lines). For the area above [below] the respective line we have $\chi_{xx}(\mathbf{R}) > \chi_{zz}(\mathbf{R})$ [$\chi_{xx}(\mathbf{R}) < \chi_{zz}(\mathbf{R})$]. Corresponding to each value of α the red dashed lines are the contour lines for $\sin^2\theta_{\rm HL} = 0.35$. The yellow area is excluded by the condition that only the lowest subband is occupied. The red star symbol indicates the point for GaAs, where for all $\varepsilon_F \gtrsim 1.2$ we have $\chi_{xx}(\mathbf{R}) > \chi_{zz}(\mathbf{R})$.

above the lines the opposite relation. The dashed lines are contour lines for $\sin^2\theta_{\rm HL} = 0.35$ associated to each value of α. As can be seen from Fig. 4, the boundary lines where the transition $\chi_{xx}(\mathbf{R}) < \chi_{zz}(\mathbf{R})$ to $\chi_{xx}(\mathbf{R}) > \chi_{zz}(\mathbf{R})$ occurs almost coincides with the corresponding contour of $\sin^2\theta_{\rm HL} = 0.35$. Figure 4 implies that an increase of the amount of HH-LH mixing also entails an increase of $\chi_{xx}(\mathbf{R})/\chi_{zz}(\mathbf{R})$ and determines the easy-axis versus easy-plane dominance of the impurity spins. Moreover, Fig. 4 shows that there is an approximately universal value for the HH-LH mixing angle $\sin^2\theta_{\rm HL} \sim 0.35$ at which the phase transition occurs. The behavior of the easy-axis versus easy-plane components of the spin susceptibility tensor can be understood intuitively by considering the influence of a in-plane magnetic field on a two-dimensional hole gas. An in-plane magnetic field has a suppressed coupling to HH states,[39,43] which in turn implies a tiny Zeeman splitting. On the contrary, the coupling of an in-plane magnetic field to LH states is not suppressed. Thus, these features of HH and LH states get interchanged when HH-LH mixing is promoted, and clearly leaves an imprint in the spin susceptibility tensor. Consequently, one could conjecture that the easy-plane components χ_{xx} and χ_{yy} are increased with respect to the easy-axis component χ_{zz} when HH-LH mixing increases. It is however worth emphasizing that the transition happens not for $\sin^2\theta_{\rm HL} \sim 0.5$, as one would naively expect from this argument, but for a much lower value.

So far we have considered the case of two isolated impurities and their exchange interaction mediated by the spin susceptibility tensor as given in Eqs. (14a)–(14d). In semiconductor systems with a high density of magnetic impurities it is useful to average over the distances of all impurities assuming that they are randomly but on average homogeneous distributed. This corresponds to taking the mean field limit in the calculation of the Curie temperature.[25] In such

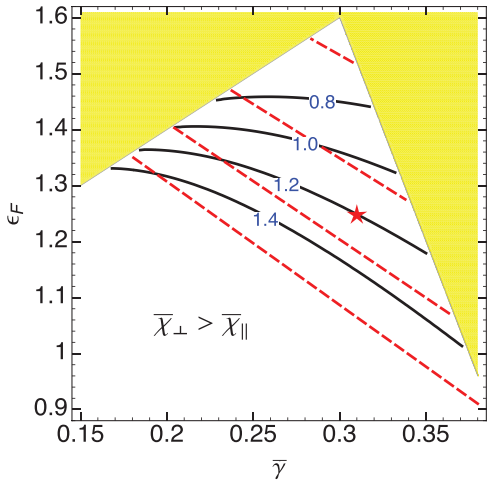

FIG. 5. (Color online) Same as in Fig. 4 but for the integrated spin susceptibility elements $\overline{\chi}_\perp$ and $\overline{\chi}_\parallel$ [Eq. (21)].

a way the discrete sum can be replaced by an integral[44]

$$\overline{\chi}_{ii} = n^{\text{imp}} \int d\mathbf{R} \chi_{ii}(\mathbf{R}), \tag{21}$$

where n^{imp} denotes the density of impurities and we define $\overline{\chi}_{zz} \equiv \overline{\chi}_\perp$ and $\overline{\chi}_{xx} = \overline{\chi}_{yy} \equiv \overline{\chi}_\parallel$ since the angular part of the in-plane components drops out after the integration over ϕ_R, see Eqs. (14a) and (14b). In Fig. 5 we show the boundary lines of $\overline{\chi}_\parallel = \overline{\chi}_\perp$ in the $\bar{\gamma}$-ε_F plane for the same values of α as in Fig. 4. Again we include the contours $\sin^2\theta_{\text{HL}} = 0.35$ as in Fig. 4. In comparison with Fig. 4, we see that an averaging over the distance leads to a distortion of the linear character of the boundary lines. This is mainly due to short distance contributions which show a different behavior. As a result, the boundary lines do not follow the linear behavior of $\sin^2\theta_{\text{HL}}$ over the whole parameter region shown. However, we still find that $\overline{\chi}_\parallel/\overline{\chi}_\perp$ is monotonically increasing with the Fermi energy ε_F and the structure parameters α and $\bar{\gamma}$, and thus is correlated with the HH-LH mixing angle. Exceptions to this behavior are found for $0.6 \lesssim \alpha \lesssim 0.8$, where an increase of $\bar{\gamma}$ does not yield larger $\overline{\chi}_\parallel/\overline{\chi}_\perp$. Clearly, also the universal behavior of Fig. 4 is lost and a transition from easy-axis to easy-plane dominance does not happen globally close to a particular value of $\sin^2\theta_{\text{HL}}$. For example, in the cases $\alpha = 1.4$ and $\bar{\gamma} \gtrsim 0.3$, the phase transition occurs at $\sin^2\theta_{\text{HL}} \sim 0.39$. Whereas for $\alpha = 0.8$, the value for $\sin^2\theta_{\text{HL}}$ can be around 0.32 to still obtain $\overline{\chi}_\parallel/\overline{\chi}_\perp > 1$.

V. SUMMARY

We have calculated and analyzed the spin susceptibility tensor of a homogeneous 2D hole gas, based on the Luttinger-model description of the lowest valence band within axial approximation. In such a way analytical results can be obtained that comprise the explicit dependence on the relevant band structure parameters. Our formulas show the important influence of HH-LH mixing on the elements of the spin susceptibility tensor. We find strong anisotropies both among the easy-plane components as well as among the easy-plane and easy-axis components. Moreover, we have pointed out that these anisotropies are intimately connected to the HH-LH mixed character of the hole states. In particular, we find that the anisotropy between easy-plane components depends only on the amount of LH character in the lowest HH-like band, characterized by $\sin^2\theta_{\text{HL}}$ [Eq. (19)]. Also, we find an almost universal value for $\sin^2\theta_{\text{HL}}$ for the switching from easy-axis to easy-plane aligned impurity spins. In contrast, we recover the well-known result of an 2DEG in the limit of zero HH-LH mixing, with impurity spins aligned perpendicular to the quantum well.

ACKNOWLEDGMENTS

The author is indebted to M. Governale, R. Winkler, and U. Zülicke for numerous helpful and interesting discussions.

[1] M. A. Rudermann and C. Kittel, Phys. Rev **96**, 99 (1954).
[2] T. Kasuya, Prog. Theor. Phys. **16**, 45 (1956).
[3] K. Yosida, Phys. Rev. **106**, 893 (1957).
[4] B. Fischer and M. W. Klein, Phys. Rev. B **11**, 2025 (1975).
[5] I. Ya. Korenblit and E. F. Shender, Zh. Eksp. Teor. Fiz. **69**, 1112 (1975) [Sov. Phys. JEPT **42**, 566 (1975)].
[6] P. Simon, B. Braunecker, and D. Loss, Phys. Rev. B **77**, 045108 (2008).
[7] H. Imamura, P. Bruno, and Y. Utsumi, Phys. Rev. B **69**, 121303 (2004).
[8] W.-M. Huang, C.-H. Chang, and H.-H. Lin, Phys. Rev. B **73**, 241307(R) (2006).
[9] P. Lyu, N.-N. Liu, and C. Zhang, J. Appl. Phys. **102**, 103910 (2007).
[10] H.-H. Lai, W.-M. Huang, and H.-H. Lin, Phys. Rev. B **79**, 045315 (2009).
[11] D. F. Mross and H. Johannesson, Phys. Rev. B **80**, 155302 (2009).
[12] S. Chesi and D. Loss, Phys. Rev. B **82**, 165303 (2010).
[13] R. A. Żak, D. L. Maslov, and D. Loss, Phys. Rev. B **82**, 115415 (2010).
[14] R. A. Żak, D. L. Maslov, and D. Loss, Phys. Rev. B **85**, 115424 (2012).
[15] L. Brey, H. A. Fertig, and S. Das Sarma, Phys. Rev. Lett. **99**, 116802 (2007).
[16] M. Sherafati and S. Satpathy, Phys. Rev. B **84**, 125416 (2011).
[17] F. Matsukura, H. Ohno, A. Shen, and Y. Sugawara, Phys. Rev. B **57**, 2037(R) (1998).
[18] G. Zaránd and B. Jankó, Phys. Rev. Lett. **89**, 047201 (2002).
[19] D. J. Priour, Jr., E. H. Hwang, and S. Das Sarma, Phys. Rev. Lett. **92**, 117201 (2004).
[20] L. Brey and G. Gómez-Santos, Phys. Rev. B **68**, 115206 (2003).
[21] G. A. Fiete, G. Zaránd, B. Jankó, P. Redliński, and C. P. Moca, Phys. Rev. B **71**, 115202 (2005).
[22] C. Timm and A. MacDonald, Phys. Rev. B **71**, 155206 (2005).

[23]T. Jungwirth, J. Sinova, J. Masek, J. Kucera, and A. H. MacDonald, Rev. Mod. Phys. **78**, 809 (2006).
[24]A. Haury, A. Wasiela, A. Arnoult, J. Cibert, S. Tatarenko, T. Dietl, and Y. M. d'Aubigné, Phys. Rev. Lett. **79**, 511 (1997).
[25]T. Dietl, A. Haury, and Y. M. d'Aubigné, Phys. Rev. B **55**, 3347(R) (1997).
[26]D. J. Priour, E. H. Hwang, and S. Das Sarma, Rhys. Rev. Lett. **95**, 037201 (2005).
[27]D. Kechrakos, N. Papanikolaou, K. N. Trohidou, and T. Dietl, Phys. Rev. Lett. **94**, 127201 (2005).
[28]R. G. Melko, R. S. Fishman, and F. A. Reboredo, Phys. Rev. B **75**, 115316 (2007).
[29]E. Z. Meilikhov and R. M. Farzetdinova, JETP Lett. **87**, 482 (2008).
[30]E. I. Rashba and E. Ya. Sherman, Phys. Lett. A **129**, 175 (1988).
[31]D. A. Broido and L. J. Sham, Phys. Rev. B **31**, 888 (1985).
[32]T. Kernreiter, M. Governale, and U. Zülicke, Phys. Rev. Lett. **110**, 026803 (2013).
[33]M. G. Pala, M. Governale, J. König, U. Zülicke, and G. Iannaccone, Phys. Rev. B **69**, 045304 (2004).
[34]B. A. Bernevig and Shou-Cheng Zhang, Phys. Rev. Lett. **95**, 016801 (2005).
[35]T. Kernreiter, M. Governale, and U. Zülicke, New J. Phys. **12**, 093002 (2010).
[36]T. Dollinger, A. Scholz, P. Wenk, R. Winkler, J. Schliemann, and K. Richter, arXiv:1304.7747.
[37]J. M. Luttinger, Phys. Rev. **102**, 1030 (1956).
[38]I. Vurgaftman, J. R. Meyer, and L. R. Ram-Mohan, J. Appl. Phys. **89**, 5815 (2001).
[39]R. Winkler, *Spin-Orbit Coupling Effects in Two-Dimensional Electron and Hole Systems* (Springer, Berlin, 2003).
[40]A. Yu. Zyuzin and B. Z. Spivak, Pis'ma. Zh. Eksp. Teor. Fiz. **43**, 185 (1986) [JETP Lett. **43**, 234 (1986)].
[41]V. I. Litvinov and V. K. Dugaev, Phys. Rev. B **58**, 3584 (1998).
[42]V. K. Dugaev, V. I. Litvinov, and P. P. Petrov, Superlattices Microstruct. **16**, 413 (1994).
[43]R. Winkler, Dimitrie Culcer, S. J. Papadakis, B. Habib, and M. Shayegan, Semicond. Sci. Technol **23**, 114017 (2008).
[44]The positional averaging done here serves as a qualitative estimate of the the easy-axis versus easy-plane behavior. It should be however noted that in order to arrive at a more quantitative estimate of this feature, subtleties in doing the sum would need to be taken into account, see for instance Refs. 20 and 21.